SCIENCE CHINA
Information Sciences

• RESEARCH PAPER •

February 2026, Vol. 69, Iss. 2, 122202:1–122202:19
https://doi.org/10.1007/s11432-024-4438-5

Towards proof-of-prospect consensus mechanism for maximizing consumers' satisfaction in distributed energy systems

Yuqi XIE[1], Changbing TANG[2*], Zhiyi CHEN[3], Jingang LAI[4],
Zhonglong ZHENG[5] & Xinghuo YU[3*]

[1]*School of Mathematical Sciences, Zhejiang Normal University, Jinhua 321004, China*
[2]*College of Physics and Electronic Information Engineering, Zhejiang Normal University, Jinhua 321004, China*
[3]*School of Engineering, Royal Melbourne Institute of Technology University, Melbourne VIC 3000, Australia*
[4]*School of Artificial Intelligence and Automation, Huazhong University of Science and Technology, Wuhan 430074, China*
[5]*School of Computer Science and Technology, Zhejiang Normal University, Jinhua 321004, China*

Received 29 October 2024/Revised 1 April 2025/Accepted 14 May 2025/Published online 10 September 2025

Abstract With economic prosperity on the rise, modern energy consumers are experiencing higher living standards and increasingly demanding greater satisfaction from energy systems, especially in scenarios involving risk. Satisfaction with risk decisions means consumers seek to make wise decisions when facing risks to optimize satisfaction. Yet, traditional optimization struggles with the increasing decentralization of energy systems, posing significant challenges to optimizing satisfaction with risk decisions. Blockchain technology, with its inherent decentralization, offers potential solutions to this challenge. However, blockchain systems encounter challenges in effectively integrating consensus mechanisms that optimize energy allocation. To fill this gap, a proof-of-prospect (PoP) consensus mechanism is presented in this paper, designed to enhance consumer satisfaction in the realm of risk decision-making. Recognizing that solutions are challenging to identify but straightforward to validate, the PoP substitutes the resource-intensive hash puzzle in the proof-of-work consensus mechanism with an optimization focused on consumer satisfaction. This shift not only boosts consumer satisfaction but also mitigates energy expenditure. Our findings indicate that in contrast to traditional consensus models, the PoP promotes fairness, decentralization, and reliability while improving consumer satisfaction and minimizing energy usage.

Keywords blockchain consensus mechanism, distributed energy systems, distributed optimization, prospect theory, risk decision, satisfaction

Citation Xie Y Q, Tang C B, Chen Z Y, et al. Towards proof-of-prospect consensus mechanism for maximizing consumers' satisfaction in distributed energy systems. Sci China Inf Sci, 2026, 69(2): 122202, https://doi.org/10.1007/s11432-024-4438-5

1 Introduction

With the global economy's expansion, the fulfillment of consumers' fundamental needs has led to an increased emphasis on their individual preferences, which directly shapes their expectations for satisfaction [1,2]. Consumers' satisfaction is a key indicator for any service, as it is directly related to customer loyalty and market reputation [3]. In energy systems, consumers' satisfaction is even more critical because it is not just about meeting basic energy needs, but also about improving quality of life, promoting environmental sustainability, and ensuring economic viability.

In the realm of energy systems, satisfaction often depends on decisions made under conditions of risk. Consumers are driven to make choices that mitigate the risks associated with energy consumption, thereby increasing their satisfaction levels [4]. For example, energy consumers must navigate the trade-offs between cost, reliability, and environmental impact, all subject to various uncertainties and risks [5–7]. However, current centralized optimization methods have limitations in optimizing satisfaction with risk decisions due to the decentralization of consumer interactions [8].

Blockchain technology provides a solution to manage collaboration systems in a decentralized manner, reducing the dependency on a central authority [9]. However, energy systems that utilize blockchain technology often treat the consensus and application layers independently, posing two significant challenges. Firstly, as a cornerstone of

* Corresponding author (email: tangcb@zjnu.edu.cn, x.yu@rmit.edu.au)

blockchain, the consensus mechanism necessitates energy for the validation process, resulting in substantial energy consumption [10]. The proof-of-work (PoW), exemplified by Bitcoin, incurs significant energy expenditure [11]. proof-of-stake [12] reduces energy use but risks centralization, while proof-of-capacity [13] improves efficiency but requires substantial storage. Secondly, energy allocation has physical limits requiring complex optimization solvers in the application layer, leading to unnecessary system operations [8]. For example, optimizing energy allocation to minimize demand charges requires extra solvers [14].

Integrating validator selection in the consensus mechanism with satisfaction optimization could tackle the two challenges. It reduces energy redundancy by replacing the centralized solver, and the energy in selecting validators is utilized to solve the satisfaction optimization problem [8]. Chen et al. [8] proposed a proof-of-solution (PoSo) consensus mechanism to integrate optimization problems. However, PoSo lacks a focus on consumer satisfaction with risk decisions. Given the core idea of integrating the consensus mechanism with satisfaction optimization problems, there are special issues that need to be addressed.

On the one hand, traditional systems narrowly measure satisfaction as a weighted assessment of economic benefits, lacking a behavioral economic theory to qualitatively characterize it with risk decisions [15]. On the other hand, psychological factors of consensus nodes affect mechanism efficiency, shaping consumer satisfaction. Current consensus mechanisms assess these factors superficially through voting, without delving into the intricate psychological behaviors through authoritative theory [16]. To accurately capture consumer satisfaction and node psychology, incorporating robust behavioral economic theories is essential.

Drawing from the previous analysis, this paper seeks to address the following two problems.

- How to design a consensus mechanism that maximizes consumer satisfaction within distributed energy systems?
- How to employ authoritative theories to measure satisfaction with risk decision-making and node psychology within consensus mechanisms?

To tackle the first problem, a proof-of-prospect (PoP) consensus mechanism is designed in this paper to optimize consumer satisfaction within the context of risk-based decision-making. The PoP consensus mechanism eliminates the computationally intensive hash puzzle from PoW, substituting it with a satisfaction optimization task that is complex to solve but simple to verify. By doing so, the PoP effectively redirects computational resources from solving meaningless puzzles to addressing problems of significance.

To address the second problem, we utilize the prospect theory (PT), as introduced by Tversky and Kahneman in 1979, which delves into how individuals make risk decisions and their resulting satisfaction levels [17]. This theory highlights that individual decision-making is influenced not only by rationality but also by psychological factors like gain-loss perception, framing effects, and personal risk attitudes. Thus, PT serves as a powerful tool to model and understand both consumers' satisfaction with risk decisions and the psychological dynamics of nodes within consensus mechanisms.

The contributions of this paper are summarized as follows.

- Diverging from prior research that predominantly hinged on economic benefits and a singular personality trait to delineate satisfaction [15, 18], this study integrates PT to formulate a multidimensional consumer satisfaction model. This model incorporates personality dimensions and psychological factors, thereby providing a nuanced depiction of consumer satisfaction.
- Unlike existing consensus mechanisms relying on voting to mirror node psychology for validator eligibility [16, 19], this paper adopts PT to develop a subjective metric, the "prospect value", as a key criterion for selecting the validator. The concept of prospect value incorporates the subjective preferences of nodes, which not only aligns with real-world scenarios but also contributes to an efficient selection process for the validator.
- After defining satisfaction and prospect value, this paper introduces a blockchain consensus mechanism that integrates satisfaction optimization, named PoP. Unlike other consensus mechanisms that predominantly consider the consensus layer [20, 21], the PoP incorporates the satisfaction optimization problem at the application layer. Initially, the PoP consensus mechanism identifies a reliable subset of nodes, forming a delegation based on their prospect values. Subsequently, the PoP selects a node from the delegation to be the validator through a satisfaction optimization process.
- We apply the PoP to the energy grid of South-Eastern Australia. We detail the satisfaction optimization problem and the operational process of the consensus mechanism in specific scenarios. The results demonstrate that the PoP can significantly enhance the satisfaction levels of consumers, and achieve a high degree of fairness while maintaining acceptable decentralization and reliability.

2 Preliminaries

In this section, we introduce the prospect theory (PT) and compare it with the expected utility theory (EUT) within risk-based decision-making. We use the example of a consumer choosing between two energy suppliers, $s1$ and $s2$, to explain the two theories. This decision is fraught with risk, as different suppliers may lead to divergent outcomes and inherent uncertainties. When selecting producer $s1$, I potential events exist, each associated with value u_i, occurring with probability p_i. Similarly, for producer $s2$, there are J potential events, each characterized by value u_j, occurring with probability p_j.

The EUT is based on choosing the option that maximizes expected utility, thus rationalizing decision-making. For producer $s1$, the expected utility, $E[s1]$, is defined as the sum of the products of each value and its corresponding probability, i.e., $E[s1] = \sum_{i=1}^{I} u_i p_i$. By analogy, for producer $s2$, the expected utility is $E[s2] = \sum_{j=1}^{J} u_j p_j$. Consequently, the consumer chooses between producers $s1$ and $s2$ based on a comparative evaluation of $E[s1]$ and $E[s2]$. The EUT offers a universal decision-making framework, assuming consistent behavior across consumers. Yet, it fails to capture the individual's unique risk attitudes and diverse preferences due to its one-size-fits-all approach. Notably, Tversky and Kahneman's seminal work reveals that decision-making is influenced by cognitive biases and behavioral tendencies [17]. This underscores the necessity for a more sophisticated model that reflects human decision-making.

The PT refines the analysis of subjective evaluations by considering potential values and probabilities, providing a nuanced framework for decision-making under uncertainty. Central to the theoretical framework of PT are the value function and the probability weighting function. The value function substitutes the value in the EUT. The value function's S-shaped curve, with a concave gain region and a convex loss region, reflects the asymmetric psychological perception of gains and losses relative to a reference point. The curve is steeper for the loss region than for the gain region, which reflects that individuals tend to amplify the perceived intensity of losses. In the case of producer $s1$, the value function that follows Tversky and Kahneman's model is [22]

$$V\left(u_i\right) = \begin{cases} \left(u_i - u^{\mathrm{e}}\right)^{\alpha}, & \text{if } u_i > u^{\mathrm{e}}, \\ -\gamma\left(u^{\mathrm{e}} - u_i\right)^{\beta}, & \text{if } u_i \leqslant u^{\mathrm{e}}, \end{cases} \tag{1}$$

where u^{e} acts as the reference point, explicitly defined as the consumer's expected value. The parameters α and β, both constrained by $0 < \alpha, \beta < 1$, capture the consumer's risk attitudes. A higher value of α and β indicates a greater propensity for the consumer to embrace risk in the pursuit of gains or in facing losses. The parameter γ quantifies the consumer's loss aversion. Specifically, $\gamma > 1$ denotes heightened sensitivity to potential losses. In the subsequent sections, the prospect value of nodes, ordinary nodes' willingness to participate in the PoP consensus mechanism, and consumer satisfaction are all modeled using the unified form of (1). This generalization is rooted in the reference-dependence principle of PT, where the definition of the reference point u^{e} in (1) is dynamically reinterpreted across scenarios. This flexibility ensures that the same theoretical framework can model decision-making contexts through scenario-driven redefinition of the reference point. The probability weighting function supplants the objective probability in the EUT with subjective weights, which reflect an individual's perception. This function tends to overstate the importance of low-probability events while understating the significance of high-probability events. For producer $s1$, the weighting function, as proposed by Prelec [23], is defined as $W\left(p_i\right) = \exp(-\left(-\ln p_i\right)^{\phi})$, where ϕ dictates how objective probabilities are translated into subjective weights by the consumer. The prospective value is derived from the product of the value function and the weighting function. For producer $s1$, the prospect value is derived from $P[s1] = \sum_{i=1}^{I} V\left(u_i\right) W\left(p_i\right)$, and similarly for producer $s2$, it is $P[s2] = \sum_{j=1}^{J} V\left(u_j\right) W\left(p_j\right)$. Ultimately, the consumer's decision between producers $s1$ and $s2$ is predicated on a comparison of $P[s1]$ and $P[s2]$, providing a nuanced approach to decision-making under risk. Despite sharing a logical basis for decision-making in uncertainty, the two theories diverge fundamentally in essence, structure, and risk preference handling. Contrasting PT with EUT in risk-based decision-making highlights PT's distinctive merits in capturing risk decision pathways that conventional EUT models fail to accommodate.

3 The principle of the PoP

The PoP consensus mechanism involves two phases: delegate formation and the validator election from the delegation, as delineated in Subsections 3.1 and 3.2. First, the system constructs prospect value attributes for nodes based on PT. These attributes reflect nodes' popularity and trustworthiness. It then forms a delegation of high-quality nodes based on prospect value to prepare for subsequent tasks. Second, the system constructs a satisfaction function based on PT and optimizes key variables to maximize consumer satisfaction. Delegates in the delegation propose solutions and the one who first proposes the optimal solution is designated as the validator. The validator, distinguished by a high prospect value and consumer trust, ensures the security of data recording. Meanwhile, the solution proposed by the validator maximizes consumer satisfaction, thereby endowing the system with strong market competitiveness. Furthermore, Subsection 3.3 delves into the incentive mechanism of the PoP consensus mechanism, aimed at maintaining the system's long-term stability.

3.1 Delegation formation

In the system, there are typically two types of interacting nodes, such as producers and consumers. Centered around one type, it treats the other as service providers. For example, when centered around consumers, producers are regarded as service providers. In this context, nodes often confront the challenge of selecting service providers. To address this challenge, node selection employs predefined criteria to evaluate each service provider. Typically, rational nodes establish their evaluation criteria based on EUT, which involves calculating the expected value for decision-making. However, due to subjective individual preferences or objective constraints in information acquisition, nodes are not fully rational. Instead, they might opt to employ PT to calculate the prospect value of service providers, thereby serving as a basis for evaluation. The prospect value represents the potential associated with each node and is used as a metric to gauge how attractive a service provider node might be for interaction. Taking the interaction between producers and consumers as an example, the system assigns a prospect value attribute to each producer based on the consumers' expected product prices and personal preferences. This attribute reflects the producer's popularity and trustworthiness among consumers. We adapt the general structure of the PT value function in (1) to the context of prospect value. Specifically, we retain the core idea of evaluating gains and losses relative to a reference point, which in this case is the expected utility $u_j^{\mathrm{e,t}}$ of node j rather than the generic reference point u^{e} in (1). The time is divided into time slots, based on the value function (1) of PT, at the t-th time slot, the prospect value of node i from the perspective of node j is

$$P_{i,j}^t = V\left(u_i^{\mathrm{e,t}}\right) = \begin{cases} \left(u_i^{\mathrm{e,t}} - u_j^{\mathrm{e,t}}\right)^{\alpha_i}, & \text{if } u_i^{\mathrm{e,t}} > u_j^{\mathrm{e,t}}, \\ -\gamma_i \left(u_j^{\mathrm{e,t}} - u_i^{\mathrm{e,t}}\right)^{\beta_i}, & \text{if } u_i^{\mathrm{e,t}} \leqslant u_j^{\mathrm{e,t}}. \end{cases} \tag{2}$$

The parameters $u_i^{\mathrm{e,t}}, u_j^{\mathrm{e,t}}$ are the expected utility of i and j, and $V(\cdot)$ is the value function of PT. Since the expected utility of node i is ascertained, the $W(\cdot)$ is omitted in $P_{i,j}^t$. $P_{i,j}^t$ is the perceived utility for node j to interact with node i, as well as the perceived acceptability of node i by node j. Assuming that each of the I nodes can interact with any one of the J nodes. Each interaction generates a prospect value which can be organized into a matrix $(P_{i,j})_{I\times J}$. Considering the previous T rounds, the cumulative prospect value for node i up to time slot t is

$$P_i^t = \sum_{l=t-T+1}^{t} l_1^{t-l} \frac{1}{J} \sum_{j=1}^{J} P_{i,j}^{l,\prime}, \tag{3}$$

where l_1 is the temporal decay factor diminishing the influence of prospect value over time and $P_{i,j}^{l,\prime} = P_{i,j}^l / \sum_{i=1}^{I} P_{i,j}^l$ normalizes the prospect values. The prospect value indicates a node's receptiveness, with nodes exhibiting high receptivity being favored for recording critical information.

Then, three indicators for PoP are identified. Indicators of fairness Fai, decentralization Dec, and reliability Rel are meticulously chosen to reflect aspects of human behavior and risk decision-making. By emphasizing these indicators, we establish a solid foundation for delegation formation. To operationalize these indicators, we define a threshold for the prospect value, denoted as P_0. The threshold operates as a selection criterion to filter a subset of candidate nodes from the node set $\mathcal{I}$.

To evaluate the fairness Fai of the PoP, we employ the Gini index, which is a standard measure of equality. In the context of PoP, it quantifies the distribution of prospect values among the nodes. We introduce a binary variable ι_k to denote whether a node's prospect value exceeds the threshold P_0. Specifically, $\iota_i = 1$ if $P_i > P_0$, and $\iota_i = 0$ otherwise. Fai is then calculated as follows:

$$\mathrm{Fai} = 1 - \frac{1}{2I\overline{\iota_i}} \sum_{i \neq i'} \sum_{i'} \left|\iota_i - \iota_{i'}\right|. \tag{4}$$

The parameter $\overline{\iota_i}$ is the average value of ι_i across $\mathcal{I}$. Building upon the assessment of fairness, we address the aspect of decentralization through the Nakamoto index, represented by Dec. This index measures the potential threats, revealing the minimum number of nodes that could compromise the integrity of the blockchain system when colluding [24]. Dec is given by

$$\mathrm{Dec} = \left|\{i \in \mathcal{I} \mid P_i \geqslant P_0\}\right| / I. \tag{5}$$

Now we consider the reliability of the PoP, denoted by Rel. Rel assesses the trustworthiness of the nodes within the delegation. The reliability is calculated using the highest $P^{\max}$ and lowest $P^{\min}$ prospect values among the applicants

$$\mathrm{Rel} = \left(P_0 - P^{\min}\right) / \left(P^{\max} - P^{\min}\right). \tag{6}$$

This formula provides a normalized measure of reliability, ensuring that delegates with higher prospect values are recognized for their potential contribution to the system's stability. All three metrics satisfy the condition $\mathrm{Fai}, \mathrm{Dec}, \mathrm{Rel} \in [0, 1]$, with higher values indicating better performance of the respective indicators. A comprehensive indicator Com is established to describe the comprehensive performance

$$\mathrm{Com} = \frac{\rho_1^2 + \rho_2^2 + (1 - \rho_1 - \rho_2)^2}{\frac{\rho_1^2}{\mathrm{Fai}} + \frac{\rho_2^2}{\mathrm{Dec}} + \frac{(1-\rho_1-\rho_2)^2}{\mathrm{Rel}}}, \tag{7}$$

where ρ_1 and ρ_2 represent the weighted importance of Fai and Dec. These weights are constrained by $\rho_1, \rho_2 \geqslant 0$, and $\rho_1 + \rho_2 \leqslant 1$, ensuring a balanced contribution of each indicator to Com.

Lastly, the threshold of prospect value P_0 is optimized to achieve a balanced assessment of the PoP and then form the delegation. P_0 is formulated as Problem 1, which seeks to maximize Com over the range of possible prospect values.

Problem 1 (Optimal prospect value threshold)**.**

$$P_0^* = \underset{P_0 \in [P^{\min}, P^{\max}]}{\mathrm{argmax}} \ \mathrm{Com}. \tag{8}$$

Nodes with a prospect value above P_0 are chosen for the delegation $\mathcal{D}$. Each delegation is dissolved at the end of its time slot, making way for a new one. Note that validators' prospect values are reset to 0 upon disbandment, other delegates' values remain, ensuring their ongoing participation in the next slot.

3.2 Validator election

The consumer satisfaction optimization function is formulated based on PT, which serves as the core objective for the application layer. This function is designed to optimize key variables (e.g., energy allocation volume) to maximize consumer satisfaction, taking into account subjective consumer perceptions. The consensus layer leverages a delegation-based mechanism where delegates propose solutions to the satisfaction optimization problem. The first delegate to propose the optimal solution is selected as the validator, ensuring that the solution is both optimal and trustworthy.

First, we construct an optimization problem to maximize consumer satisfaction based on their expectations and personalized parameters. Even when confronted with the same outcomes, the perceived satisfaction may vary significantly due to differences in their expectations and personalized parameters [25]. The satisfaction of consumers is fundamentally shaped by PT's value function, which quantifies how consumers perceive outcomes relative to their expectations. Specifically, consumer j's satisfaction S_j is determined by objective utility, expected utility, and personalized parameters. Objective utility $u_j(\boldsymbol{x})$ is the actual utility derived from the decision vector $\boldsymbol{x}$ (e.g., energy allocation volume). Expected utility u_j^{e} is the consumer's subjective reference point, which serves as a psychological benchmark. Personalized parameters $\alpha_j, \beta_j, \gamma_j$ are the coefficients capturing risk attitudes and loss aversion as defined in (1). Consumer j's satisfaction function S_j integrates these elements through the function $V(\cdot)$ defined in (1). The resulting satisfaction function is given by

$$S_j(\boldsymbol{x}) = V\left(u_j(\boldsymbol{x})\right) = \begin{cases} \left(u_j(\boldsymbol{x}) - u_j^{\mathrm{e}}\right)^{\alpha_j}, & \text{if } u_j(\boldsymbol{x}) > u_j^{\mathrm{e}}, \\ -\gamma_j \left(u_j^{\mathrm{e}} - u_j(\boldsymbol{x})\right)^{\beta_j}, & \text{if } u_j(\boldsymbol{x}) \leqslant u_j^{\mathrm{e}}, \end{cases} \tag{9}$$

where the explicit form of $u_j(\boldsymbol{x})$ depends on application-specific factors, such as energy consumption patterns or financial incentives. Similar to (1), Eq. (9) applies the PT value function to measure consumer j's satisfaction. The reference point here is the expected utility u_j^{e}, analogous to the reference point u^{e} in (1) but specific to the consumer's expectations. Eq. (9) directly maps the prospect value to satisfaction measurement. The total consumer satisfaction aggregates individual satisfaction across all J consumers

$$S_{\text{total}}(\boldsymbol{x}) = \sum_{j=1}^{J} S_j(\boldsymbol{x}). \tag{10}$$

Formally, we formulate the optimization Problem 2 to maximize total consumer satisfaction within the feasible region $\boldsymbol{X}$.

Problem 2 (Maximize satisfaction)**.**

$$\boldsymbol{x}^* = \underset{\boldsymbol{x}\in\boldsymbol{X}}{\operatorname{argmax}} S_{\text{total}}(\boldsymbol{x}). \tag{11}$$

Then, each member of the delegation has the right to propose solutions to Problem 2 within T_1 seconds. The member who first presents an optimal solution earns the role of validator. We claim the members of the delegation as delegates. The collective set of solutions from delegation $\mathcal{D}$ is denoted as $\boldsymbol{x}_{\mathcal{D}} = \{\boldsymbol{x}_d | d \in \mathcal{D}\}$. Verifiers, denoted by $b \in \mathcal{B}$, receive and validate the solutions proposed by the delegates. The PoP incorporates reliable broadcast (RBC) and asynchronous binary agreement (ABA) principles to ensure all verifiers reliably receive the delegate solutions [26].

If Problem 2 is convex or concave, verifiers can use the Karush-Kuhn-Tucker (KKT) conditions to identify the optimal solution within the set $\boldsymbol{x}_{\mathcal{D}}$. The first delegate to submit the optimal solution is appointed as the validator. For non-convex/non-concave Problem 2, verifiers assess the objective values of $S_{\text{total}}(\boldsymbol{x})$ to determine the best solution. If $\boldsymbol{x}_d$ stands out among $\boldsymbol{x}_{\mathcal{D}}$, then d is the validator. It is worth noting that $\boldsymbol{x}_d$ is relatively optimal with respect to the set $\boldsymbol{x}_{\mathcal{D}}$, and may not be globally optimal.

3.3 Incentive model

Consensus is the key to stability in distributed systems, yet it is threatened by minimal node involvement. The PoP addresses this by incentivizing nodes with block reward R, which is derived from collective transaction fees. It is critical to adjust R to prevent the rewards from being too meager, which could demotivate nodes, or too generous, which could overburden the nodes and undermine system sustainability.

We denote the participation willingness of ordinary node k in the consensus process as h_k. Building on this, we extend the value function of PT, as presented in (1), to quantify the willingness of node k to participate in the consensus process

$$h_k = V(u_k) = \begin{cases} (u_k - u_k^{\mathrm{e}})^{\alpha_k}, & \text{if } u_k > u_k^{\mathrm{e}}, \\ -\gamma_k (u_k^{\mathrm{e}} - u_k)^{\beta_k}, & \text{if } u_k \leqslant u_k^{\mathrm{e}}. \end{cases} \tag{12}$$

It maintains the fundamental structure of evaluating outcomes relative to a reference point, with u_k^{e} representing the expected utility of node k for participating in the consensus process. This is similar to the reference point u^{e} in (1) but tailored to the specific scenario of consensus participation. The term $u_k = p_k R - \mu_k$ is the actual utility in the consensus process, where the parameter p_k is the probability of node k receiving the block reward, and μ_k is the commission fee. The commission paid by the nodes is $\mu_k = \varepsilon\zeta_k R$, where ε is the commission rate and ζ_k is the transaction volume.

To optimize the system, we define the set of ordinary nodes as $\mathcal{K}$ and seek to maximize the total willingness among all ordinary nodes, $\sum_{k\in\mathcal{K}} h_k$, leading to the following optimization problem.

Problem 3 (Optimal block reward)**.**

$$R^* = \underset{R}{\operatorname{argmax}} \sum_{k\in\mathcal{K}} h_k.$$

Theorem 1 delineates the optimal solution to Problem 3, establishing the optimal reward for the system.

Theorem 1. Given that ordinary nodes possess positive utility, there exists a unique optimal block reward, denoted as R^*. This optimal reward is derived from the following equation:

$$R^* = u_k^{\mathrm{e}} / (p_k - \varepsilon\zeta_k). \tag{13}$$

Proof. Given that ordinary nodes achieve a positive utility, we have $u_k = p_k R - \mu_k = p_k R - \varepsilon\zeta_k R > 0$. Given that $R \geqslant 0$, it follows that $\varepsilon < p_k/\zeta_k$. We define $\mathcal{K}_{\text{high}}$ as the subset of ordinary nodes for which $u_k > u_k^{\mathrm{e}}$, with the remaining ordinary nodes comprising the set $\mathcal{K}_{\text{low}}$. Then, the sum of willingness is

$$\sum_{k\in\mathcal{K}} h_k = \sum_{k\in\mathcal{K}_{\text{high}}} h_k + \sum_{k\in\mathcal{K}_{\text{low}}} h_k. \tag{14}$$

Given the h_k defined in (12), for $k \in \mathcal{K}_{\rm high}$, we have $h_k = (u_k - u_k^{\rm e})^{\alpha_k}$, where $u_k = p_k R - \mu_k$ and $\mu_k = \varepsilon\zeta_k R$. First, we compute the first derivative of u_k with respect to R for $k \in \mathcal{K}_{\rm high}$

$$\frac{\partial u_k}{\partial R} = \frac{\partial\left(p_k R - \varepsilon\zeta_k R\right)}{\partial R} = p_k - \varepsilon\zeta_k.$$

Next, we define H as $H = \sum_{k\in\mathcal{K}_{\rm high}} h_k$, and then compute the first derivative of H with respect to R

$$\frac{\partial H}{\partial R} = \sum_{k\in\mathcal{K}_{\rm high}} \alpha_k \left(u_k - u_k^{\rm e}\right)^{\alpha_k - 1} \frac{\partial u_k}{\partial R} = \sum_{k\in\mathcal{K}_{\rm high}} \alpha_k \left(u_k - u_k^{\rm e}\right)^{\alpha_k - 1} \left(p_k - \varepsilon\zeta_k\right).$$

To find the second derivative of H with respect to R, we differentiate $\frac{\partial H}{\partial R}$. Thus, we obtain $\frac{\partial^2 H}{\partial R^2}$ as

$$\frac{\partial^2 H}{\partial R^2} = \sum_{k\in\mathcal{K}_{\rm high}} \alpha_k \left(\alpha_k - 1\right)\left(u_k - u_k^{\rm e}\right)^{\alpha_k - 2} \left(p_k - \varepsilon\zeta_k\right)^2. \tag{15}$$

Eq. (15) characterizes the degree of curvature of h_k to R. Since $0 < \alpha_k < 1$ and $u_k > u_k^{\rm e}$, the term on the right-hand side of (15) is less than 0. Given that the feasible region for the block reward R is convex, a unique optimal solution R exists for Problem 3. The first derivative of h_k indicates its slope of change. Setting the first-order partial derivative of h_k with respect to 0

$$\frac{\partial H}{\partial R} = \sum_{k\in\mathcal{K}_{\rm high}} \alpha_k \left(u_k - u_k^{\rm e}\right)^{\alpha_k - 1} \left(p_k - \varepsilon\zeta_k\right) = 0. \tag{16}$$

Given that $\varepsilon < p_k/\zeta_k$, $p_k > 0$, and $\alpha_k > 0$, we have

$$\alpha_k \left(u_k - u_k^{\rm e}\right)^{\alpha_k - 1} \left(p_k - \varepsilon\zeta_k\right) \geqslant 0, \forall k \in \mathcal{K}_{\rm high}. \tag{17}$$

Thus, Eq. (16) holds true if and only if $p_k R - \varepsilon\zeta_k R - u_k^{\rm e} = 0$, for $k \in \mathcal{K}_{\rm high}$. Hence, $R^* = u_k^{\rm e}/\left(p_k - \varepsilon\zeta_k\right)$ is satisfied for $k \in \mathcal{K}_{\rm high}$. For the second term on the right-hand side of (14), since $u_k \leqslant u_k^{\rm e}$ and h_k increases with increasing R, it is derived that $R^* \leqslant u_k^{\rm e}/\left(p_k - \varepsilon\zeta_k\right), \forall k \in \mathcal{K}_{\rm low}$. Consequently, $R^* = u_k^{\rm e}/\left(p_k - \varepsilon\zeta_k\right)$ is also satisfied for $k \in \mathcal{K}_{\rm low}$. The proof is complete.

Remark 1. Different ordinary nodes will have different values for $u_k^{\rm e}/\left(p_k - \varepsilon\zeta_k\right)$. To maximize the participation willingness across the system, R^* is set as the median of these values.

Remark 2. Adhering to the principle of individual rationality, nodes must derive a positive utility from their engagement in the consensus mechanism. This requirement establishes the condition that ε must satisfy $\varepsilon < \min_{k\in\mathcal{K}} p_k/\zeta_k$, ensuring a fair and sustainable incentive structure.

4 Apply the PoP to energy allocation

In this section, we employ the PoP consensus mechanism for energy allocation, detailing two primary steps as outlined in Subsections 4.1 and 4.2. The comprehensive methodology of PoP within energy allocation is further explained in Subsection 4.3.

Our energy allocation network comprises both application and consensus layers, as illustrated in Figure 1. Our system focuses on the flow of energy from producers to consumers, with electricity as the exchange medium. The system includes three types of entities: producers, prosumers, and consumers. Producers have large-scale power generation equipment, while consumers rely entirely on purchasing electricity. Prosumers own small-scale power generation devices and act as either producers or consumers in the energy allocation system based on their generation minus consumption during a specific period. If their generation exceeds consumption, they are producers; otherwise, they are consumers. Thus, only producers and consumers are present in the system at any given time. The utility grid is crucial for electricity transmission from producers to consumers. Producers are enabled to actively participate as delegates and are eligible for block rewards, enhancing their market engagement. Energy allocation is quantified in discrete time slots, each from one midnight to the next. For simplicity, we will refer to time t only when necessary. In the application layer, the key task is addressing the satisfaction optimization problem, contingent upon the decision variable of allocation volume. In the consensus layer, validators are tasked with uploading allocation data to the blockchain, ensuring data security and system transparency. The novelty of our proposed PoP is its dual functionality: it determines allocation volumes and guides validator elections. This dual role strengthens the synergy between allocation and validator selection, enhancing the blockchain system's performance and reliability.

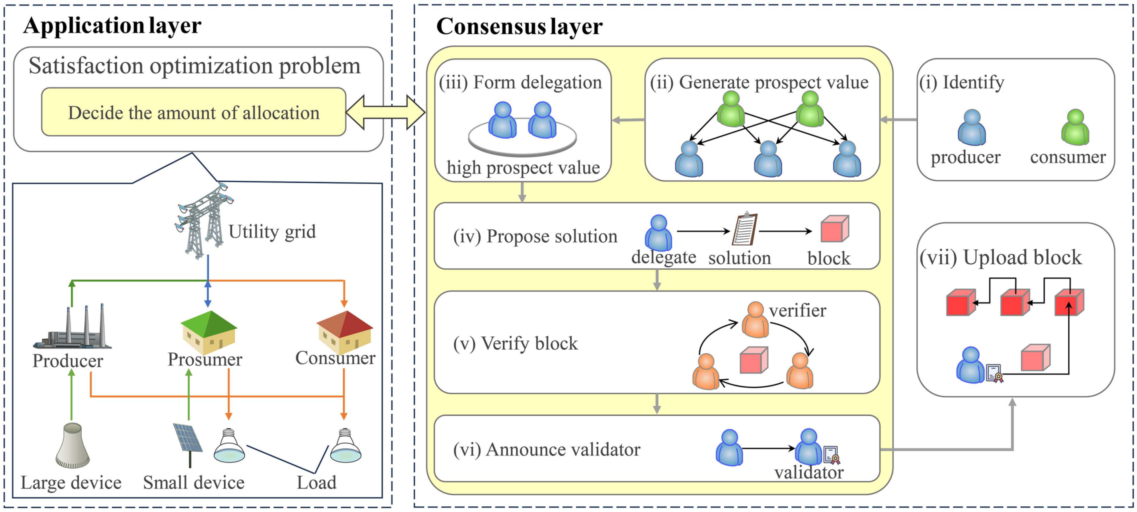

Figure 1 (Color online) System architecture.

4.1 Delegation formation in energy allocation

Firstly, each producer is assigned a prospect value that reflects risk-based decision-making in energy allocation. The producers are represented by index i, and the consumers by j. Price is recognized as the main driver of consumer behavior [27], and thus, the prospect value is derived from expected electricity prices. From the perspective of consumer j, the prospect value $P_{i,j}$ associated with producer i under PT is defined by the value function $V(\cdot)$ in (1), specifically

$$P_{i,j} = V\left(p_i^{\text{sup}}\right) = \begin{cases} \left(p_i^{\text{sup}} - p_j^{\text{dem}}\right)^{\alpha_j}, & \text{if } p_i^{\text{sup}} > p_j^{\text{dem}}, \\ -\gamma_j \left(p_j^{\text{dem}} - p_i^{\text{sup}}\right)^{\beta_j}, & \text{if } p_i^{\text{sup}} \leqslant p_j^{\text{dem}}, \end{cases} \tag{18}$$

where p_i^{sup} denotes the expected electricity supply price (ESP) of producer i, and p_j^{dem} is the expected electricity demand price (EDP) of consumer j. Eq. (18) generalizes the formulation of (1) by contextualizing its reference point u^{e} as the p_j^{dem} in energy allocation. Consumer preference for lower prices leads to an inversion of p_j^{dem} and p_i^{sup} in (18) compared to (2). The value $P_{i,j}$ indicates the degree of consumer j's acceptance of producer i based on price. Subsequently, the delegation formation process follows as described in Subsection 3.1.

4.2 Validator election in energy allocation

In our proposed PoP consensus mechanism, the satisfaction optimization function and the blockchain consensus mechanism are tightly integrated to achieve a balance between consumer satisfaction and consensus security. In an energy allocation system, the satisfaction optimization function aims to maximize consumer satisfaction by optimizing the volume of energy allocated to each consumer. The consensus layer, comprising a delegation of trusted producer nodes, evaluates proposed solutions based on their ability to achieve this optimization goal. The node that proposes the solution with the highest consumer satisfaction value is selected as the validator, responsible for recording the transaction data. This integration ensures that the consensus process is driven by consumer-centric optimization while maintaining the security and reliability of the blockchain.

Individuals frequently assess their actual utility by comparing it with expected utility, a process that is closely linked to both their historical utility and the utility of their peers [28]. This comparative assessment of utility significantly influences an individual's life satisfaction. Drawing from this insight, we introduce a "satisfaction" metric that accounts for individual personality traits and social dynamics. In this study, application-layer producers establish their ESPs and, as consensus-layer delegates, propose solutions to optimize satisfaction. The first delegate to propose an optimal solution is rewarded with a block reward. This solution also dictates the volume of allocated energy.

Firstly, an optimization problem aimed at maximizing consumer satisfaction in energy allocation is constructed. The utility function of consumer j is given by

$$U_j(\boldsymbol{x}) = q_j \ln\left(\max\left(\sum_{i=1}^{I} \delta_j x_{i,j} - E_j^{\min}, 0\right) + 1\right) - \sum_{i=1}^{I} \delta_j r_{i,j} x_{i,j}$$

$$-\max\left(E_j^{\min}-\sum_{i=1}^{I}\delta_j x_{i,j},\,0\right)r^{\rm off}-\sum_{i=1}^{I}|d_i^{\rm geo}-d_j^{\rm geo}|x_{i,j}. \tag{19}$$

The term $\boldsymbol{x}=(x_{i,j})_{I\times J}$ represents the optimization variable in (19). The primary component in (19) measures consumer benefits derived from electricity purchases [29]. The following two terms calculate consumer j's electricity costs sourced from energy producers and the utility grid. The final component is the grid's transmission fee, representing the cost of using the grid's infrastructure for electricity allocation. The willingness to purchase electricity for j is indicated by $q_j=\tau/\omega_j$, with τ a constant and ω_j signifying the surplus electricity accessible to consumer j. The variable $x_{i,j}$ represents the electricity allocated from producer i, corresponding to the received electricity $y_{i,j}$ of consumer j. The equation $y_{i,j}=\delta_j x_{i,j}$ defines this relationship, with δ_j indicating the transfer efficiency. The parameter $E_j^{\min}$ denotes the minimum volume of electricity that consumer j wishes to receive. The logarithmic function $\ln(\cdot+1)$ captures the diminishing marginal utility phenomenon, where incremental gains in $\delta_j x_{i,j}$ yield progressively less satisfaction, aligning with Gossen's first law of economics [30]. The $+1$ term avoids undefined logarithmic operations at 0 allocation levels and reflects the baseline utility for consumers. The electricity price $r_{i,j}$ negotiated between i and j is determined by $r_{i,j}=\left(p_i^{\rm sup}+p_j^{\rm dem}\right)/2+\varpi\sum_{j=1}^{J}E_j^{\min}$, where ϖ is a constant. To promote local electricity consumption, we set the expected prices, $p_i^{\rm sup}$ and $p_j^{\rm dem}$, within the bounds $[r^{\rm on},r^{\rm off}]$. Here, $r^{\rm on}$ represents the on-grid tariff at which producers sell electricity to the grid, while $r^{\rm off}$ denotes the off-grid tariff at which consumers purchase electricity from the grid. Thus, the price of purchasing electricity from the grid is $r^{\rm off}$. The third term represents the additional electricity consumer j must obtain from the grid when the producer's supply is insufficient. The term $\left|d_i^{\rm geo}-d_j^{\rm geo}\right|x_{i,j}$ denotes the transmission fee levied on consumers by the utility grid. This cost is related to the transmission distance $\left|d_i^{\rm geo}-d_j^{\rm geo}\right|$ and the volume of electricity transmitted $x_{i,j}$. The values of $d_i^{\rm geo}$ and $d_j^{\rm geo}$ are correlated with the geographical locations of producer i and consumer j. The expected utility of consumer j at time slot t is $U_j^{\rm e}=\overline{U_{j'}^{t}}+\frac{1}{t-1}\sum_{l=1}^{t-1}\left(U_j\right)^l$, which is related to the utility of other consumers and their historical $t-1$ time slots utility. In accordance with (9), the satisfaction function for consumer j is mathematically expressed as $S_j(\boldsymbol{x})=V\left(U_j(\boldsymbol{x})\right)$. Subsequently, the total satisfaction of all consumers is

$$S_{\rm total}(\boldsymbol{x})=\sum_{j=1}^{J}S_j(\boldsymbol{x}). \tag{20}$$

In conjunction with (11), the consumer-centric satisfaction optimization challenge in the energy allocation systems can be rigorously expressed as the following constrained maximization problem.

Problem 4 (Maximize satisfaction in energy allocation)**.**

$$\max_{\boldsymbol{x}}\ S_{\rm total}(\boldsymbol{x}) \tag{21}$$

$$z_i^{\min}\leqslant x_{i,j}\leqslant z_i^{\max},\forall i\in\mathcal{I}, \tag{22}$$

$$z_j^{\min}\leqslant \delta_j x_{i,j}\leqslant z_j^{\max},\forall j\in\mathcal{J}, \tag{23}$$

$$\sum_{j=1}^{J}x_{i,j}\leqslant E_i^{\max},\forall i\in\mathcal{I}. \tag{24}$$

The parameters $z_i^{\min}$ and $z_i^{\max}$ are the minimum and maximum energy transmissible of producer i, respectively, and $z_j^{\min}$ and $z_j^{\max}$ are the minimum and maximum energy transmissible of consumer j, respectively. Constraints (22) and (23) ensure that the transferred electricity remains within the operational transmissible capacity of the producers and consumers. $E_i^{\max}$ is the maximum electricity supply of producer i. Constraint (24) stipulates that the allocated quantity does not exceed the maximum supply capability. Theorem 2 implies the complexity of finding the optimal solution, which requires various optimization algorithms.

Theorem 2. The satisfaction maximization Problem 4 is characterized by both supermodularity and submodularity.

Proof. A function $F(x,y)$ is considered supermodular if, for all $x_1>x_2$ and $y_1>y_2$, the following inequality holds

$$F(x_1,y_1)+F(x_2,y_2)\geqslant F(x_1,y_2)+F(x_2,y_1). \tag{25}$$

We introduce an auxiliary function $g(\lambda)$ defined as

$$g(\lambda)=F\left(\lambda x_1+(1-\lambda)x_2,\lambda y_1+(1-\lambda)y_2\right),$$

where $\lambda \in [0,1]$. This function effectively interpolates between the points (x_1, y_1) and (x_2, y_2). Applying the mean value theorem to $g(\lambda)$, which is continuous on $[0,1]$ and differentiable on $(0,1)$, ensures the existence of some $\lambda^* \in (0,1)$ such that $g'(\lambda^*) = g(1) - g(0)$. Here, $g(1) = (x_1, y_1)$ and $g(0) = (x_2, y_2)$. For the supermodularity condition $g(1) \geqslant g(0)$ to hold, it is necessary that $g'(\lambda^*) \geqslant 0$. By computing the derivative of $g(\lambda)$ with respect to λ, we obtain

$$\begin{aligned} g'(\lambda) = & \frac{\partial F}{\partial x}(\lambda x_1 + (1-\lambda) x_2, \lambda y_1 + (1-\lambda) y_2)(x_1 - x_2) + \frac{\partial F}{\partial y}(\lambda x_1 + (1-\lambda) x_2, \lambda y_1 \\ & + (1-\lambda) y_2)(y_1 - y_2). \end{aligned}$$

Evaluating this at λ^*, we see that the condition $g'(\lambda^*) \geqslant 0$ is dominated by the sign of the cross partial derivative $F(x,y)/\partial x \partial y$. Specifically, for $g'(\lambda^*) \geqslant 0$ to hold for all $x_1 > y_1$ and $x_2 > y_2$, it is required that $F(x,y)/\partial x \partial y \geqslant 0$. Thus, if $F(x,y)$ is differentiable, Eq. (25) is equivalent to the non-negativity of its cross partial derivative [31]:

$$\frac{F(x,y)}{\partial x \partial y} \geqslant 0.$$

Conversely, $F(x,y)$ is deemed submodular if the cross partial derivative is non-positive. To demonstrate that the function Problem 4 exhibits both supermodular and submodular properties, it suffices to establish that $V(u)$ is neither convex nor concave to U_j^t. We are to prove that the function

$$V(u) = \begin{cases} (u - u^{\mathrm{e}})^{\alpha}, & \text{if } u > u^{\mathrm{e}}, \\ -\gamma (u^{\mathrm{e}} - u)^{\beta}, & \text{if } u \leqslant u^{\mathrm{e}} \end{cases}$$

is neither convex nor concave to u. Taking the second derivative of the function $V(u)$ with respect to u yields

$$\partial^2 V(u)/\partial u^2 = \begin{cases} \alpha(\alpha-1)(u - u^{\mathrm{e}})^{a-2}, & \text{if } u > u^{\mathrm{e}}, \\ -\gamma\beta(\beta-1)(u^{\mathrm{e}} - u)^{\beta-2}, & \text{if } u \leqslant u^{\mathrm{e}}. \end{cases}$$

Given that $0 < \alpha, \beta < 1$ and $\gamma > 0$, we have

$$\begin{cases} \partial^2 V(u)/\partial u^2 < 0, & \text{if } u > u^{\mathrm{e}}, \\ \partial^2 V(u)/\partial u^2 > 0, & \text{if } u \leqslant u^{\mathrm{e}}. \end{cases}$$

This signifies that the point $(u^{\mathrm{e}}, V(u^{\mathrm{e}}))$ identifies an inflection point for the function $V(u)$. Beyond this point, for $u > u^{\mathrm{e}}$, $V(u)$ exhibits upward convexity, whereas for $u \leqslant u^{\mathrm{e}}$, it demonstrates downward concavity. Consequently, function $V(u)$ is both non-convex and non-concave concerning u, which makes Problem 4 inherently supermodular and submodular. This settles the proof.

For the non-convex non-concave Problem 4, we derive the KKT conditions as necessary conditions for local optimality of a candidate solution $\boldsymbol{x} = (x_{i,j})_{I \times J}$. These conditions help identify potential local optima, though further verification is required to confirm optimality. The KKT conditions consist of

$$\left.\frac{\partial \mathcal{L}}{\partial \boldsymbol{x}}\right|_{\boldsymbol{x}=\boldsymbol{x}^*} = 0, \tag{26a}$$

$$r^{\mathrm{T}} \left.\frac{\partial^2 \mathcal{L}}{\partial \boldsymbol{x}^2}\right|_{\boldsymbol{x}=\boldsymbol{x}^*} r > \mathbf{0}, \forall r \neq 0, \tag{26b}$$

$$G_i^l\left(\boldsymbol{x}^*, \Xi^{G_i}\right) \leqslant 0, \forall i \in \mathcal{I}, l = 1,2,3, \tag{26c}$$

$$G_j^l\left(\boldsymbol{x}^*, \Xi^{G_j}\right) \leqslant 0, \forall j \in \mathcal{J}, l = 4,5, \tag{26d}$$

$$\varphi_i^{l,*} G_i\left(\boldsymbol{x}^*, \Xi^{G_i}\right) = 0, \forall i \in \mathcal{I}, l = 1,2,3, \tag{26e}$$

$$\chi_j^{l,*} G_j\left(\boldsymbol{x}^*, \Xi^{G_j}\right) = 0, \forall j \in \mathcal{J}, l = 4,5, \tag{26f}$$

$$\varphi_i^{l,*} \geqslant 0, \forall i \in \mathcal{I}, l = 1,2,3, \tag{26g}$$

$$\chi_j^{l,*} \geqslant 0, \forall j \in \mathcal{J}, l = 4,5, \tag{26h}$$

$\mathcal{L}$ represents the Lagrange function of Problem 4. $\varphi_i^{l,*}$ and $\chi_j^{l,*}$ are lagrange multipliers. r is an auxiliary vector, $G_i^1(\boldsymbol{x}) = x_{i,j} - z_i^{\min}$, $G_i^2(\boldsymbol{x}) = z_i^{\max} - x_{i,j}$, $G_i^3(\boldsymbol{x}) = \sum_{j=1}^{J} x_{i,j} - E_i^{\max}$, $G_j^4(\boldsymbol{x}) = \delta_j x_{i,j} - z_i^{\min}$, and $G_j^5(\boldsymbol{x}) =$

$z_i^{\max} - \delta_j x_{i,j}$. Due to the complexity of sub-formulas (26a) and (26b), we focus on conducting a deep analysis of them.

Given the function $S_{\text{total}}(\boldsymbol{x})$ defined as $S_{\text{total}}(\boldsymbol{x}) = \sum_{j=1}^{J} S_j(\boldsymbol{x})$. The Lagrangian equation $\mathcal{L}$ for Problem 4 is given as

$$\mathcal{L} = \sum_{j=1}^{J} S_j(\boldsymbol{x}) + \sum_{i\in\mathcal{I}} (\varphi_i^{1,*}(x_{i,j} - z_i^{\min}) + \varphi_i^{2,*}(z_i^{\max} - x_{i,j}))$$
$$+ \sum_{i\in\mathcal{I}} \varphi_i^{3,*} \left(E_i^{\max} - \sum_{j=1}^{J} x_{i,j} \right) + \sum_{j\in\mathcal{J}} (\chi_j^{4,*}(\delta_j x_{i,j} - z_j^{\min}) + \chi_j^{5,*}(z_j^{\max} - \delta_j x_{i,j})),$$

where

$$S_j(\boldsymbol{x}) = V(U_j(\boldsymbol{x})),$$

and $U_j(\boldsymbol{x})$ is defined in (19).

The first-order derivative of the $\mathcal{L}$ with respect to $\boldsymbol{x}$ is given by

$$\partial\mathcal{L}/\partial\boldsymbol{x} = g_1(\boldsymbol{x}) L1(\boldsymbol{x}) + \sum_{i=1}^{I} \varphi_i^1 - \sum_{i=1}^{I} \varphi_i^2 + \sum_{i=1}^{I} \varphi_i^3 + \sum_{j=1}^{J} \chi_j^1 \delta_j - \sum_{j=1}^{J} \chi_j^2 \delta_j, \tag{27}$$

where

$$g_1(\boldsymbol{x}) = \begin{cases} -\alpha \left(U_j(\boldsymbol{x}) - U_j^{\mathrm{e}} \right)^{\alpha-1}, & j \in \mathcal{J}_{\text{high}}, \\ -\gamma\beta \left(U_j^{\mathrm{e}} - U_j(\boldsymbol{x}) \right)^{\beta-1}, & j \in \mathcal{J}_{\text{low}}, \end{cases}$$

$\mathcal{J}_{\text{high}}$ and $\mathcal{J}_{\text{low}}$ are the consumer sets with utility above and below expectation, respectively, and

$$L1(\boldsymbol{x}) = \frac{\beta_j \delta_j}{\sum_{j=1}^{J} \delta_j x_{i,j} - E_j^{\min} + 1} - r_{i,j} + \delta_j r^{\text{off}} - \left| d_i^{\text{geo}} - d_j^{\text{geo}} \right|.$$

Here, r^{off} denotes the unit price of electricity purchased from the power grid, as defined in (19). Eq. (26a) implies that at $\boldsymbol{x} = \boldsymbol{x}^*$, the determinant of the matrix composed of elements specified by (27) is 0. The second partial derivative of $\mathcal{L}$ with respect to $\boldsymbol{x}$ is given by

$$\partial^2\mathcal{L}/\partial\boldsymbol{x}^2 = g_2(\boldsymbol{x}) L_1(\boldsymbol{x})^2 + g_1(\boldsymbol{x}) \left(\frac{\beta_j \delta_j^2}{\left(\sum_{j=1}^{J} \delta_j x_{i,j} - E_j^{\min} + 1 \right)^2} \right), \tag{28}$$

where

$$g_2(\boldsymbol{x}) = \begin{cases} -\alpha (\alpha - 1) \left(u_j(\boldsymbol{x}) - U_j^{\mathrm{e}} \right)^{\alpha-2}, & j \in \mathcal{J}_{\text{high}}, \\ -\gamma\beta (\beta - 1) \left(U_j^{\mathrm{e}} - U_j(\boldsymbol{x}) \right)^{\beta-2}, & j \in \mathcal{J}_{\text{low}}. \end{cases}$$

Eq. (26b) indicates that at $\boldsymbol{x} = \boldsymbol{x}^*$, the matrix with elements given by (28) is positive definite. In summary, a feasible solution $\boldsymbol{x}^*$ must satisfy the KKT conditions in (26) to be a candidate for local optimality in Problem 4. However, due to the non-convexity of Problem 4, these conditions alone do not guarantee local optimality. To confirm $\boldsymbol{x}^*$ as a local optimum, additional analysis (e.g., verifying the positive definiteness of the Hessian on the tangent space or comparing the objective function values) is required to exclude saddle points and higher-order critical points.

Then, delegates within the delegation are tasked with proposing solutions to Problem 4. The delegate who first submits the optimal solution earns the role of validator, consequently receiving block rewards from the consensus layer. However, since these delegates also engage in energy allocation as producers, the proposed solution inherently impacts their utility within the application layer. Selfish delegates are not solely focused on finding the optimal solution to Problem 4; they are motivated to propose a solution that maximizes the combined utility from electricity allocation and block reward. Therefore, we analyze the selfish delegates' overall utility.

Let delegate $d \, (d \in \mathcal{D})$ propose solution $\boldsymbol{x}_d$. We consider the dual role of delegate d as producer i. Producer i gains utility from the electricity allocation defined by $U_i(\boldsymbol{x}) = \sum_{j=1}^{J} r_{i,j} x_{i,j} + (E_i^{\max} - \sum_{j=1}^{J} x_{i,j}) r^{\text{on}}$. The first term represents earnings from consumers, while the second reflects the revenue from interactions with the utility grid. Here, the term $E_i^{\max}$ denotes the maximum electricity supply of producer i. The overall utility for delegate

Algorithm 1 Process of the PoP in energy allocation.

Input: Set of expected utility U^{e}, Problem 4.
Output: Validator d^*.
Stage 1: Form delegation $\mathcal{D}$ in energy allocation.
1: Calculate prospect value P_i by (3);
2: Calculate Fai, Dec, and Rel by (4)–(6);
3: Obtain P_0 by (8);
4: **if** $P_i > P_0$ **then** $\mathcal{D} \leftarrow \mathcal{D} \cup i$;
5: **end if**
Stage 2: Elect validator d^* in energy allocation.
6: Delegate d proposes solutions $\boldsymbol{x}_d$;
7: Verifier b receives solutions set $\boldsymbol{X}_b$;
8: **if** solution $\boldsymbol{x}_d$ satisfies the conditions for the optimal solution of Problem 4 **then** Delegate d^* is the validator;
9: **else** Keep $\boldsymbol{x}_d$ if $\boldsymbol{x}_d = \mathrm{argmax}_{\boldsymbol{X}_b} S_{\mathrm{total}}(\boldsymbol{x})$;
10: **end if**
11: Broadcast $\boldsymbol{x}_d$ to neighbor nodes;
12: Verifier b updates $\boldsymbol{X}_b$;
13: Repeat steps 7–12 until all nodes keep $\boldsymbol{x}_d$;
14: Delegate d^* is the validator.

d is articulated as $U_d(\boldsymbol{x}) = \mathrm{val}_d R + U_i(\boldsymbol{x}^*)$, where the binary variable val_d indicates whether delegate d serves as the validator. When $\boldsymbol{x}_d = \boldsymbol{x}^*$, d acts as a validator with $\mathrm{val}_d = 1$, and thus d is eligible to receive the block reward R. Therefore, selfish validators balance the block reward R against the utility function $U_i(\boldsymbol{x})$ to achieve the maximum overall benefit $U_d(\boldsymbol{x})$. In contrast, altruistic validators simply aim to propose solutions that optimize Problem 4. The block reward is closely connected to the dynamics of power generation within the electricity system. When there is a surplus of new renewable energy generation, a larger block reward is engineered to incentivize the use of renewable sources. Conversely, in scenarios with predominant thermal power generation, the block reward is reduced. The nodes selected by the PoP exhibit both altruism and a broader perspective, which is crucial for ensuring the smooth operation of the consensus mechanism and preventing potential issues like system forks.

4.3 Process of the PoP in energy allocation

In the realm of consensus mechanisms, the validator plays a pivotal role in overseeing the system's state, while the PoP consensus mechanism extends this by addressing the energy allocation optimization in a decentralized manner. The workflow of PoP is outlined and depicted in Figure 1, with a detailed procedural breakdown provided in Algorithm 1.

(i) **Identify.** Nodes within the energy system are classified as either producers or consumers, predicated on their projected electricity generation and consumption. Producer $i\,(i = 1, \ldots, I)$ engages with the system by proposing p_i^{sup} and $E_i^{\max}$. In turn, consumer $j\,(j = 1, \ldots, J)$ communicates energy demands to the system by specifying p_j^{dem} and $E_j^{\min}$.

(ii) **Generate prospect value.** The prospect value for each producer is gained, drawing on data provided by producers and consumers. This value encapsulates the collective subjective judgments of consumers, reflecting the producer's acceptance within the energy system (Algorithm 1 step 1).

(iii) **Form delegation.** A threshold for the prospect value is established to form a delegation. Producers whose prospect values surpass this threshold become delegates and have the authority to propose solutions to the satisfaction maximization problem (Algorithm 1 steps 2–5).

(iv) **Propose block.** The energy system's overarching goal is to optimize consumer satisfaction, which is formulated at the application layer. It considers societal objectives and consumer subjective choices. Each delegate proposes a block that includes their solutions (Algorithm 1 step 6).

(v) **Verify block.** Verifiers receive and validate the block, which includes verifying the correctness of the transaction information and ensuring that the solution satisfies the KKT conditions of Problem 4. Each validator b receives a set of solutions $\boldsymbol{X}_b$ from neighboring nodes. If an optimal solution is present in the set, the validator propagates this solution to its neighbors via a peer-to-peer network. (Algorithm 1 steps 7–13).

(vi) **Announce validator.** The delegate who first proposes the optimal solution is selected as the validator. If no delegate proposes the optimal solution, the system selects the best alternative solution from those proposed by the delegation, and the delegate who proposed this solution is the validator. The solution of the validator directs the energy allocation volumes between prosumers (Algorithm 1 step 14).

(vii) **Upload block.** The validator's approved block is then uploaded to the main blockchain, integrating the new data into the existing ledger.

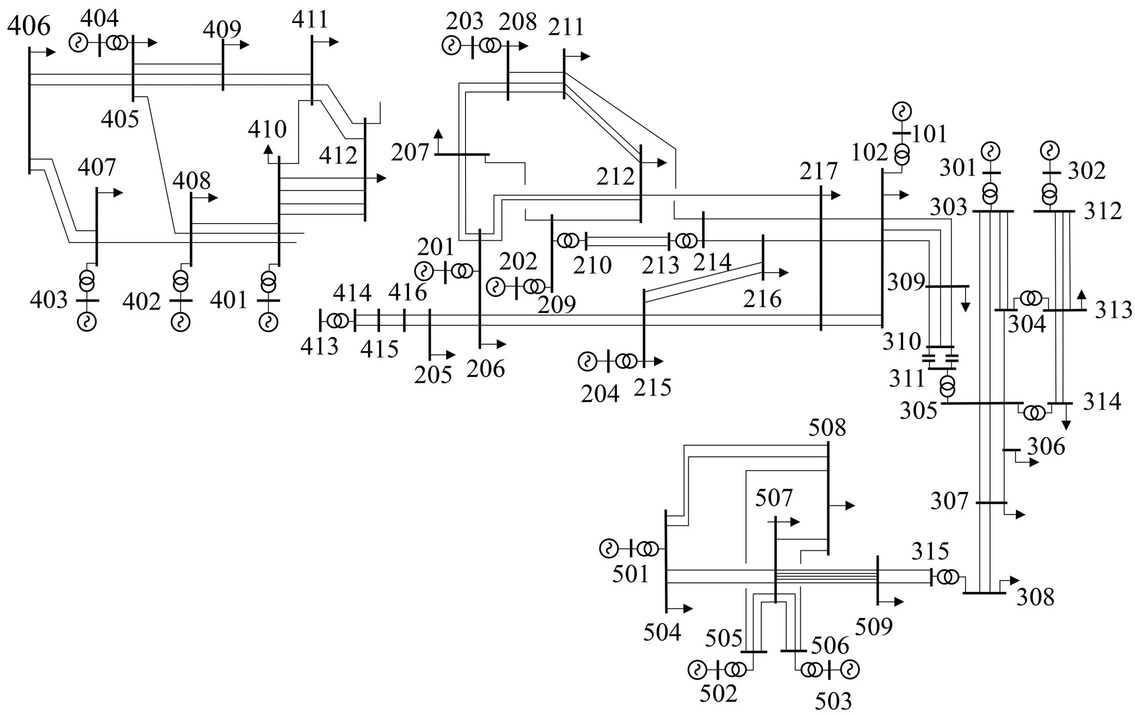

Figure 2 Simplified 14-generator Australian power grid.

5 Simulation

In this section, we substantiate the feasibility of the PoP and assess its performance through its application to a simplified South-Eastern Australian energy system model. The simplified model is shown in Figure 2. Adhering to the regional electricity pricing norms of South-Eastern Australia, the paper adopts the unit c/kW·h for electricity pricing, signifying Australian cents per kilowatt-hour. The parameters required for experiment initialization are provided in Tables B1 and B2 of Appendix B. The system aims to optimize consumer satisfaction, thereby bolstering market competitiveness. The model differentiates between altruistic producers who strive to enhance the system's objectives and selfish producers whose primary goal is the maximization of their benefits. Our approach involves the strategic selection of a subset of producers to serve as delegates, and we hope that this process will ensure fairness, decentralization, and reliability of the PoP. Subsequently, we aim to appoint a delegate to serve as the validator, and the validator proposes solutions to maximize consumer satisfaction.

5.1 Delegation formation in energy allocation

First, we evaluate how the personality parameters of Australian consumers affect the prospect value of producers, as depicted in Figures 3(a) and (b). For this analysis, we consider a consumer with an EDP set at 10 c/kW·h, reflecting the average electricity prices in Australia. Figure 3(a) illustrates the variation in producer's ESP, ranging from 5 to 15 c/kW·h, and their corresponding prospect value. Figure 3 reveals an inverse ESP-prospect value correlation: higher ESPs correspond to lower prospect values, aligning with PT's value function. This implies that consumers tend to favor producers with lower ESPs. When the ESP deviates from the consumer's EDP, the prospect value correlates with different personality parameters. Specifically, if the ESP is below the EDP, the prospect value is influenced by the parameter α, which indicates the consumer's risk-taking propensity for potential gains. Conversely, if the ESP exceeds the EDP, the parameters β and γ come into play. Here, β reflects the consumer's risk-taking propensity for avoiding losses, and γ is the loss aversion coefficient, signifying the consumer's heightened sensitivity to losses over gains. The effect of α and β on the prospect value is opposite: a higher α leads to a higher prospect value, while a higher β results in a lower prospect value. The effect of parameter γ on the prospect value is similar to that of β.

Next, we explore the likelihood of producers accessing the delegation by comparing their prospect values to the threshold, as illustrated in Figure 4. We categorize producers into three types based on their ESP ranges: Type A with ESPs between 9 and 11 c/kW·h, Type B between 11 and 13 c/kW·h, and Type C between 13 and 15 c/kW·h.

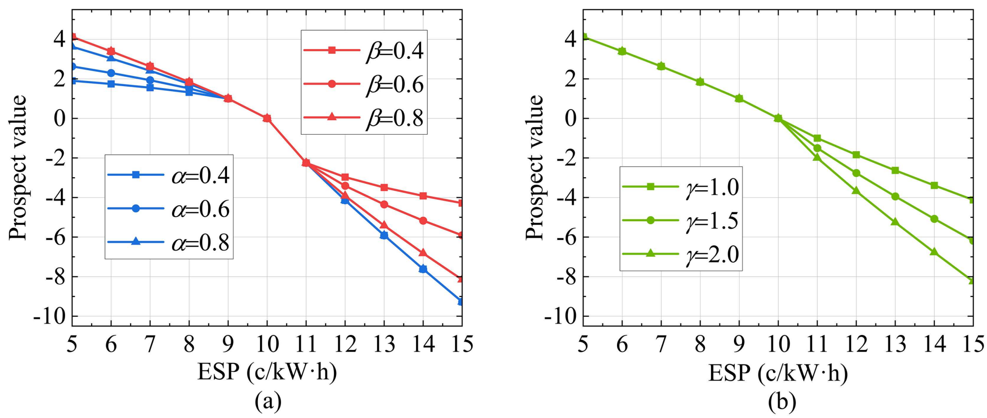

Figure 3 (Color online) Prospect values of producers. (a) Prospect values with different α and β; (b) prospect values with different γ.

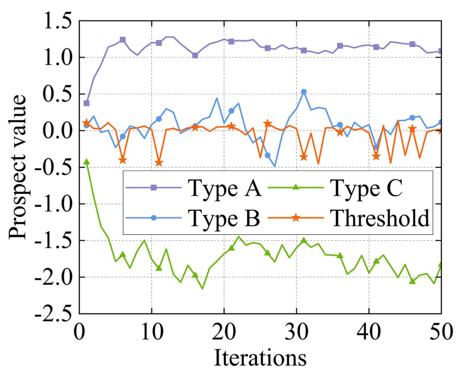

Figure 4 (Color online) Comparison of prospect values with the threshold.

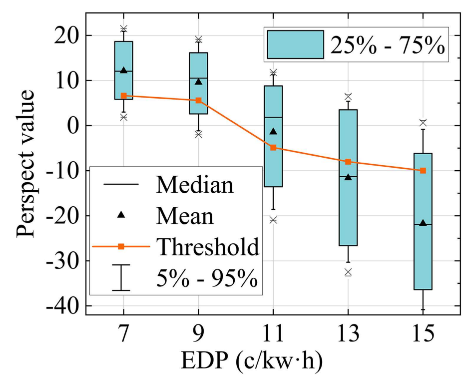

Figure 5 (Color online) Prospect values and prospect value thresholds.

Our analysis indicates that Type A and Type B producers have prospect values above the threshold, suggesting higher delegation access for those with lower ESPs. This observation suggests a correlation between the ESP and their potential to become delegates.

Finally, we present the prospect value threshold against a backdrop of fluctuating EDP values, ranging from 7 to 15 c/kW·h, as shown in Figure 5. Within this figure, the blue box demarcates the threshold, with the median prospect value indicated by a black horizontal line and the mean prospect value signified by a black triangular marker. As the EDP increases, the threshold value gradually approaches and eventually surpasses both the mean and median prospect values. Initially, at lower EDP levels, the threshold is below both the mean and median. However, as EDP rises, the threshold value increases and intersects with the mean and median prospect values. Beyond this intersection point, the threshold continues to rise and remains above both the mean and median, indicating a growing disparity between the threshold and the central tendency measures of the prospect values. This phenomenon indicates that the threshold is positively correlated with EDP. As EDP increases, the threshold rises accordingly, which increases the difficulty for producers to delegate, thereby ensuring the reliability of the delegation.

This trend can be attributed to the decline in overall prospect values, necessitating an elevated threshold to uphold the reliability of the consensus process.

5.2 Validator election in energy allocation

Here, we simulate the solution proposal process for delegates with varying motivations using grey wolf optimization (GWO) [32] and particle swarm optimization (PSO) [33]. The GWO uses wolf pack dynamics as an optimization model, emphasizing hierarchical leadership in search strategies. PSO simulates social behaviors such as bird flocks and finds the best solution through the cooperative movement of particles. The main difference between the two is that GWO focuses on hierarchical hunting, while PSO focuses on collective intelligence in group behavior. Selfish Delegate A and altruistic Delegate B utilize GWO, yielding Solutions A and B. Similarly, selfish Delegate C and

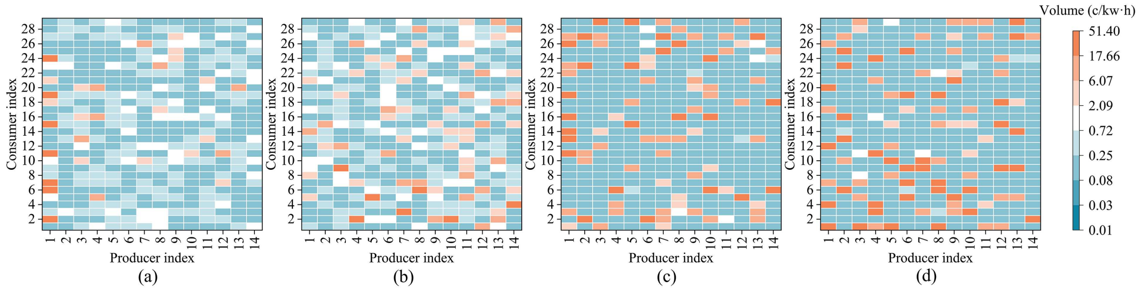

Figure 6 (Color online) The solutions. (a) Solution A (selfish, GWO); (b) solution B (altruistic, GWO); (c) solution C (selfish, PSO); (d) solution D (altruistic, PSO).

altruistic Delegate D employ PSO to produce Solutions C and D.

The comparative analysis of the proposed solutions is presented in Figure 6, where each solution is represented as a matrix. The color coding—orange for higher values and blue for lower ones—facilitates the visual differentiation of the solutions' characteristics. The visual representation in Figure 6 reveals that the GWO algorithm yields solutions with greater stability and uniformity in element values.

Further, Figure 7 illustrates the dynamic process of solution proposal by the two types of delegates using their respective algorithms. The selfish delegates are denoted by triangle markers, while the altruistic delegates are indicated by square markers. The blue curves correspond to the outcomes of the GWO algorithm, and the red curves to those of the PSO algorithm. This comparative study provides valuable insights into the behavior of different optimization algorithms under the influence of varying delegate motivations. It offers a deeper understanding of their respective strengths and potential applications in solving satisfaction optimization problems.

Finally, we outline the contrasting goals of selfish and altruistic delegates within an optimization model. Selfish delegates aim to maximize personal utility, while altruistic ones seek to improve overall consumer satisfaction. We aim to choose a validator from four delegates. The satisfaction and utility comparison among the four proposed solutions is shown in Figure 8. The delegate whose solution yields the highest satisfaction is elected as the validator and receives the block reward. In this scenario, Delegate B is selected as the validator, as the proposed solution B earns the highest satisfaction of all consumers, rather than maximizing individual utility. Since Delegate D also exhibits altruistic characteristics, the proposed optimization solution can significantly enhance the overall satisfaction and utility levels. The solutions obtained by Delegate B and Delegate D differ in terms of satisfaction and utility, as B employs the GWO while D uses the PSO algorithm. In the absence of Delegate B, Delegate D could have been selected as the validator, as the solution proposed by D achieved the second-highest level of consumer satisfaction after B. The graph also shows that selfish delegates (A and C) are not selected as validators, highlighting the PoP's effectiveness in preventing their election and reducing potential security risks. This study thoroughly explores the balance between individual incentives and collective welfare, providing insights into validator selection and the impact of their decisions on system performance and security.

5.3 Performance of the PoP

In this subsection, we evaluate the performance of the proposed PoP consensus mechanism, examining its fairness, decentralization, reliability, security, energy consumption, and applicability.

First, we evaluate and compare the fairness Fai, decentralization Dec, and reliability Rel of the PoP consensus mechanism against PoSo and delegated proof-of-stake (DPoS), as illustrated in Figure 9. Notably, DPoS is operational on both the EOS and Asch platforms [34]. In PoSo, validators are directly elected by the entire node system, precluding the delegation process. Conversely, DPoS initiates with a selection of nodes to form a delegation, from which a validator is chosen through voting. Despite the procedural variations, both the PoSo and DPoS attain a reliability metric of 1, whereas PoP exhibits a reliability of 0.650. PoSo also assigns optimization tasks to individual nodes. However, having only one node solve the problem leads to a significantly low fairness value of 0.0233 and decentralization of 0.2000. On the other hand, the EOS and Asch platforms display varying degrees of fairness (0.1846 and 0.1061 respectively) due to differences in the total and delegated node counts. The participatory nature of DPoS in voting confers a decentralization level of 0.660, marginally higher than PoP's 0.558. While PoP may not excel in reliability and decentralization compared to the other two consensus mechanisms, it maintains commendable standards within the context of distributed blockchain-enabled energy allocation systems. Moreover, PoP's fairness stands at 0.500, tripling the fairness of other consensus mechanisms.

Subsequently, Figure 10 shows the verification time for the proposed PoP consensus mechanism. Since Problem

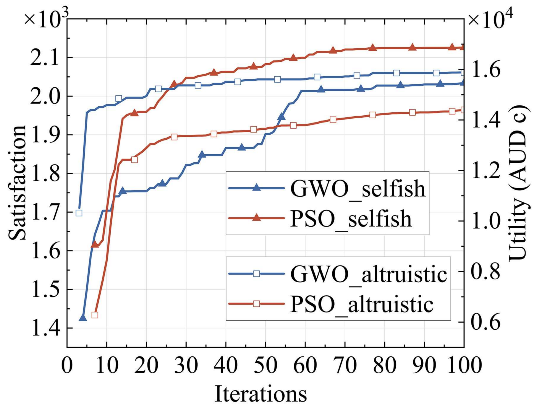

Figure 7 (Color online) Iterative process of the solutions proposed by delegates.

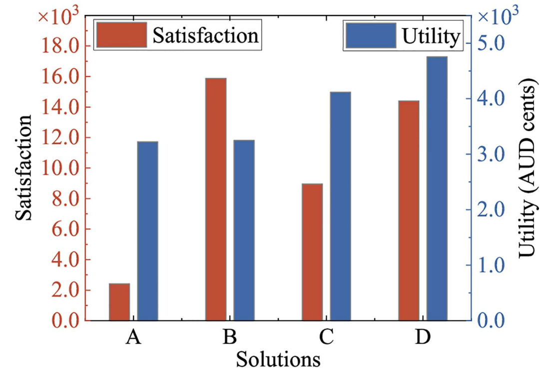

Figure 8 (Color online) Satisfaction and utility corresponding to the four solutions.

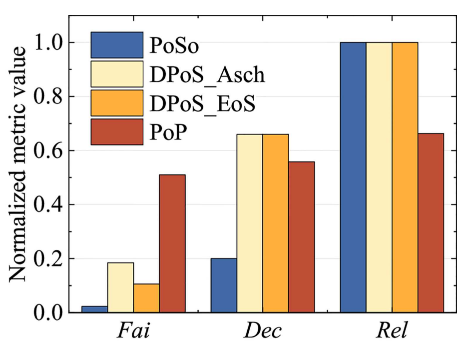

Figure 9 (Color online) The Fai, Dec, and Rel of the PoSo, DPoS, and the PoP.

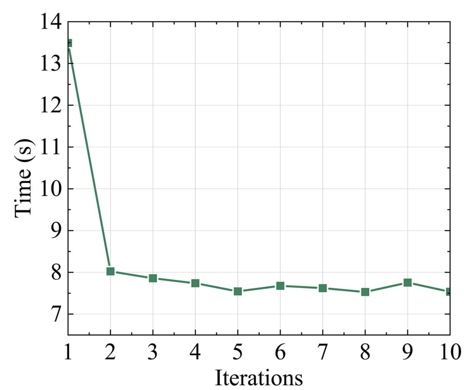

Figure 10 (Color online) Verification time required for the PoP.

4 is neither convex nor concave, verifiers must evaluate function values across all gathered solutions. The initial verification was completed in 13.5 s, with subsequent validations averaging 7.5 s each. This highlights the efficiency of PoP in terms of verification time.

Then, we validate the security of the PoP consensus mechanism by analyzing its design principles and the results shown in Figure 11. The design principles of PoP prioritize security, which encompasses both reliability and decentralization. The high-reliability standard ensures that selected validators are entrusted with the critical role of data security. Meanwhile, decentralization is fortified by the requirement for a significant node consensus to facilitate collusion, thereby enhancing overall system security. We introduce a novel security index that captures the equilibrium between reliability and decentralization, while imposing a mild penalty on deviations from an optimal decentralization level. The index is defined as $\mathrm{Sec} = 1-|\mathrm{Rel} - \mathrm{Dec}|-0.2\,|\mathrm{Dec} - 0.2|$. The security metric ranges from 0 to 1, with values approaching 1 indicating enhanced protocol security. As shown in Figure 11, the proposed PoP consensus mechanism maintains security levels between 0.8 and 1.0 (mean = 0.93, dashed line) across network scales from 1 to 1000 nodes, demonstrating robust security preservation under dynamic node variations. Furthermore, we incorporate RBC and ABA to ensure comprehensive solution dissemination among all verifiers. RBC ensures the dependable propagation of messages, while ABA specializes in achieving consensus in an asynchronous setting, particularly concerning the endorsement or rejection of proposals. In addressing the common challenge of system forking, validators within PoP are established as trustworthy entities that adhere to system protocols, preempting malicious actions. If a fork does occur, the system's security is preserved through robust voting mechanisms that identify and eliminate non-compliant nodes.

Afterward, Figure 12 validates the low energy consumption of the PoP consensus mechanism and compares it with other mechanisms. The energy consumption is minimized in our PoP consensus mechanism by avoiding solving the meaningless puzzle in PoW. The delegation formation in PoP is dictated by a threshold derived from solving Problem 1, characterized by a singular objective function, two linear constraints, and requiring minimal energy

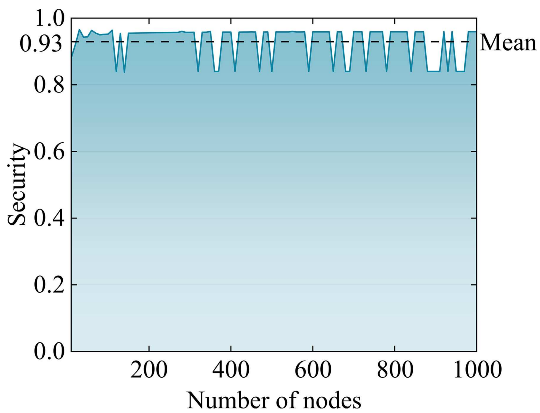

Figure 11 (Color online) Security index of PoP.

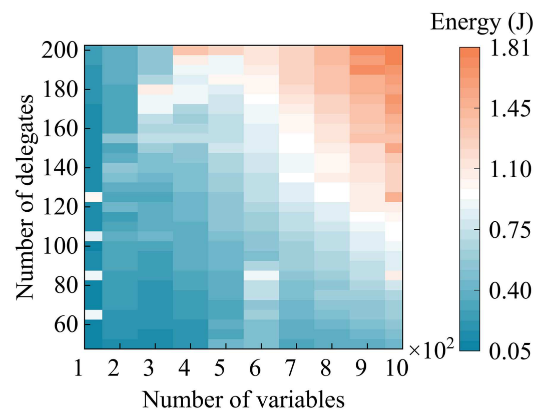

Figure 12 (Color online) Energy profile: number of delegates and variables.

Table 1 Analysis of consensus mechanism variants.

	PoW	PoSo	PoP
Fairness	High	Low	High
Decentralization	High	Low	High
Reliability	High	Medium	High
Computational workload	High	Medium	Low
Computational efficiency	Low	High	High
Combing optimization problems	No	Yes	Yes
Reflecting risk decision of nodes	No	No	Yes

to resolve. The PoP further streamlines energy use by leveraging user-provided solution verification within the delegation. Utilizing the KKT complementary conditions, this verification process is more efficient than solving the original problem, underscoring PoP's commitment to energy conservation. Figure 12 shows the energy consumption of the PoP consensus mechanism per transaction is less than 2 J. By analyzing the annual energy consumption data provided by the Cambridge Centre for Alternative Finance and the annual transaction volume data available on the official website, we estimate the energy consumption per transaction for blockchain and Ethereum to be 920 and 13.36 kW·h, respectively (the relevant data resources are listed in Appendix A). This indicates that the PoP consensus mechanism has the potential to significantly reduce energy consumption.

Furthermore, we demonstrate the applicability of the PoP mechanism through complexity analysis and simulation results. The PoP consensus mechanism exhibits a linear time complexity of $O(n)$, with n denoting the number of nodes. This highlights its scalability across various environments with a high density of nodes. Figure 12 illustrates the energy consumption of the PoP consensus mechanism as the number of optimization variables ranges from 100 to 1000, corresponding to an increase in the number of delegates from 60 to 100. The figure clearly shows that energy consumption increases with the rise in both the number of optimization variables and delegates. However, even with 1000 optimization variables and 100 delegates, the energy consumption does not exceed 2 J, underscoring the applicability of the proposed PoP consensus mechanism. Moreover, the PoP consensus mechanism is well-suited for systems with subjective participants aiming to maximize user satisfaction, with each participant's state being resolved through an optimization problem. This is particularly relevant in energy systems, such as in energy allocation and market management scenarios. In the context of energy allocation, the PoP allocates energy between producers and consumers by maximizing satisfaction, considering that all parties involved have personal perspectives and make decisions in the face of risk.

Additionally, we contrast the optimization objectives that integrate individual differences and social factors with those focused solely on economic utility. The experimental results show that the economic utility stands at 3247c and the satisfaction is 15880. Economic utility, a pivotal determinant of human satisfaction, is often translated into satisfaction through weighting in scientific and engineering domains. Even if the economic utility were to be fully converted to satisfaction, it would not surpass the levels achieved within our model. This result highlights the dual efficacy of our PoP in enhancing customer satisfaction and preserving consumer utility.

Finally, Table 1 compares the PoW, the PoSo, and our proposed PoP consensus mechanisms. The PoW is recognized for its fairness, decentralization, and reliability due to its reliance on computationally intensive hash puzzles. The PoSo and the PoP are both designed to optimize problems that lack decomposable structures. The PoSo elects a single delegate to address optimization problems, while the PoP encourages collective members to contribute to solving the problem and compete for rewards. In the PoSo, the leader is assigned to tackle the optimization problem in 220 s, followed by a verification conducted by the followers in 1 s. The PoP requires all members to submit solutions within an adjustable time frame based on transaction volume. Our tests show the PoP's average verification time is about 7.5 s, slightly longer than PoSo. Compared to PoW, the PoSo and PoP are less computationally demanding. Ethereum's PoW takes 15 s, while Bitcoin's takes 10 min. The PoW has the highest workload, followed by the PoSo, with the PoP being the least demanding. The PoP's efficiency is highlighted by its focus on solving optimization problems rather than puzzles. Furthermore, delegations are formed by prospect value, which is a social attribute based on risk decisions. This approach not only promotes a fair and strong consensus mechanism but also aligns with blockchain's decentralization.

6 Conclusion

With improving living standards, enhancing consumer satisfaction in energy allocation, particularly in the complex domain of risk decision-making for energy prosumers, is becoming increasingly important. The increasing decentralization of interactions between energy prosumers in energy systems renders traditional centralized optimization methods ineffective. This has driven the exploration of solutions within distributed energy systems, positioning blockchain technology as a key solution. Consensus mechanism is a pivotal component of blockchain technology, playing a crucial role in its architecture. In blockchain-based energy systems, the design of consensus mechanisms often involves the separation of the consensus layer from the energy application layer. This approach can lead to increased system complexity and a concomitant rise in energy consumption. In this paper, we introduce an innovative consensus mechanism termed PoP, which prioritizes consumer satisfaction based on risk decision-making. The design of PoP integrates energy allocation in the application layer, ensuring that the determination of the consensus validator is concurrent with the allocation of energy resources. This integrated approach not only simplifies the system architecture but also contributes to reduced energy consumption, enhancing the efficiency and transparency of energy allocation. The study is structured to first elucidate the theoretical principle of PoP, followed by its application in the scenario of a simplified South-Eastern Australian power grid. Our findings underscore the PoP's efficacy, demonstrating enhanced consumer satisfaction, fairness, decentralization, and reliability, while significantly reducing the energy consumption associated with consensus reaching. This not only validates the feasibility of the PoP but also highlights its potential to redefine energy allocation in distributed systems. The limitations of the PoP consensus mechanism primarily lie in its restricted application domains. In future work, we aim to focus on extending the PoP consensus mechanism to broader fields, such as supply chain management and peer-to-peer networks.

Acknowledgements This work was supported by National Natural Science Foundation of China (Grant No. 62272419) and Natural Science Foundation of Zhejiang Province (Grant Nos. LZ24F030009, LZ22F020010).

Supporting information Appendixes A and B. The supporting information is available online at info.scichina.com and link.springer.com. The supporting materials are published as submitted, without typesetting or editing. The responsibility for scientific accuracy and content remains entirely with the authors.

References

1 Oliveira C, Botelho D F, Soares T, et al. Consumer-centric electricity markets: a comprehensive review on user preferences and key performance indicators. Electric Power Syst Res, 2022, 210: 108088
2 Nambi S N A U, Prasad R V. Toward the development of a techno-social smart grid. IEEE Commun Mag, 2016, 54: 202–209
3 Giese J L, Cote J A. Defining consumer satisfaction. Acad Mark Sci Rev, 2000, 4: 1–24
4 Parag Y, Sovacool B K. Electricity market design for the prosumer era. Nat Energy, 2016, 1: 16032
5 Zhao M, Zhang C, Hu Y, et al. Modelling consumer satisfaction based on online reviews using the improved Kano model from the perspective of risk attitude and aspiration. Tech Economic Dev Economy, 2021, 27: 550–582
6 Li C, Yu X, Yu W, et al. Distributed event-triggered scheme for economic dispatch in smart grids. IEEE Trans Ind Inf, 2016, 12: 1775–1785
7 Li C, Dong Z, Chen G, et al. Data-driven planning of electric vehicle charging infrastructure: a case study of Sydney, Australia. IEEE Trans Smart Grid, 2021, 12: 3289–3304
8 Chen S, Mi H, Ping J, et al. A blockchain consensus mechanism that uses proof of solution to optimize energy dispatch and trading. Nat Energy, 2022, 7: 495–502
9 Nakamoto S. Bitcoin: a peer-to-peer electronic cash system. 2008. https://ondoc.logand.com/d/4354/pdf
10 Zhou S, Li K, Xiao L, et al. A systematic review of consensus mechanisms in blockchain. Mathematics, 2023, 11: 2248
11 Lasla N, Al-Sahan L, Abdallah M, et al. Green-PoW: an energy-efficient blockchain proof-of-work consensus algorithm. Comput Netws, 2022, 214: 109118
12 Saleh F, Jiang W. Blockchain without waste: proof-of-stake. Rev Financial Studies, 2021, 34: 1156–1190
13 Dziembowski S, Faust S, Kolmogorov V, et al. Proofs of space. In: Proceedings of Advances in Cryptology, 2015. 585–605
14 Nottrott A, Kleissl J, Washom B. Energy dispatch schedule optimization and cost benefit analysis for grid-connected, photovoltaic-battery storage systems. Renew Energy, 2013, 55: 230–240

15 Tan L, Liu N, Sun H, et al. A cyber-physical-social system approach for peer-to-peer energy sharing. IEEE Trans Smart Grid, 2024, 15: 4010–4022
16 Xu G, Liu Y, Khan P W. Improvement of the DPOS consensus mechanism in blockchain based on vague sets. IEEE Trans Ind Inf, 2020, 16: 4252–4259
17 Kahneman D, Tversky A. Prospect theory: an analysis of decision under risk. Econometrica, 1979, 47: 263–292
18 Li J, Li T, Dong D Y. Demand response management of smart grid based on Stackelberg-evolutionary joint game. Sci China Inf Sci, 2023, 66: 182201
19 Castro M, Liskov B. Practical byzantine fault tolerance. In: Proceedings of Symposium on Operating Systems Design and Implementations, 1999. 173–186
20 Wang E K, Liang Z, Chen C M, et al. PoRX: a reputation incentive scheme for blockchain consensus of IIoT. Future Generation Comput Syst, 2020, 102: 140–151
21 Kang J, Xiong Z, Niyato D, et al. Toward secure blockchain-enabled internet of vehicles: optimizing consensus management using reputation and contract theory. IEEE Trans Veh Technol, 2019, 68: 2906–2920
22 Tversky A, Kahneman D. Advances in prospect theory: cumulative representation of uncertainty. J Risk Uncertainty, 1992, 5: 297–323
23 Prelec D. The probability weighting function. Econometrica, 1998, 66: 497–527
24 Lin Q W, Li C, Zhao X F, et al. Measuring decentralization in Bitcoin and Ethereum using multiple metrics and granularities. In: Proceedings of International Conference on Data Engineering Workshops, 2021. 80–87
25 Peterson R A, Wilson W R. Measuring customer satisfaction: fact and artifact. J Acad Market Sci, 1992, 20: 61–71
26 Bracha G. Asynchronous byzantine agreement protocols. Inf Comput, 1987, 75: 130–143
27 So K K F, Oh H, Min S. Motivations and constraints of Airbnb consumers: findings from a mixed-methods approach. Tourism Manage, 2018, 67: 224–236
28 Tella R D, MacCulloch R J, Oswald A J. The macroeconomics of happiness. Rev Economics Stat, 2003, 85: 809–827
29 Bao Z, Tang C B, Lin F L, et al. Rating-protocol optimization for blockchain-enabled hybrid energy trading in smart grids. Sci China Inf Sci, 2023, 66: 159205
30 Jolink A, van Daal J. Gossen's laws. History Political Economy, 1998, 30: 43–50
31 Foldes S, Hammer P L. Submodularity, supermodularity, and higher-order monotonicities of pseudo-boolean functions. Math OR, 2005, 30: 453–461
32 Mirjalili S, Mirjalili S M, Lewis A. Grey wolf optimizer. Adv Eng Softw, 2014, 69: 46–61
33 Zhao J, Han C Z, Wei B. Binary particle swarm optimization with multiple evolutionary strategies. Sci China Inf Sci, 2012, 55: 2485–2494
34 Li C, Palanisamy B. Comparison of decentralization in DPoS and PoW blockchains. In: Proceedings of Blockchain-International Conference on Blockchain, 2020. 18–32